國立交通大學

生醫工程研究所

碩 士 論 文

根據輻射基底函數發展非剛性變形系統及
於生醫影像對位之應用

A Software System Developed based on the
Radial-Basis-Functions and Its Applications to
Biomedical Images

研 究 生：黃彥淳

指導教授：荊宇泰　教授

中 華 民 國　九 十 八 年 八 月

根據輻射基底函數發展非剛性變形系統及於生醫影像對位之應用

A Software System Developed based on the Radial-Basis-Functions and Its Applications to Biomedical Images

研 究 生：黃彥淳　　Student：Yen-Chuen Huang

指導教授：荊宇泰　　Advisor：Yu-Tai Ching

國 立 交 通 大 學

生 醫 工 程 研 究 所

碩 士 論 文

A Thesis

Submitted to Institute of Biomedical Engineering

College of Computer Science

National Chiao Tung University

in partial Fulfillment of the Requirements

for the Degree of

Master

in

Computer Science

August 2009

Hsinchu, Taiwan, Republic of China

中華民國九十八年八月

根據輻射基底函數發展非剛性變形系統及於生醫影像對位之應用

學生：黃彥淳　　指導教授：荊宇泰　博士

國立交通大學生醫工程研究所

摘　　要

為了針對生醫影像處理，使影像對位至恰當的位置，以利後續生物醫學研究，我們建立了一個交談式的視窗介面，依照已知經驗與知識，選擇特定控制點來控制影像中一些具有特徵的點能夠匹配在一起，進而達成高效能的對位結果。影像對位的演算法則是採用輻射基底函數作為能達到局部變形效果的方法，再配合全域的多項式函數，最終能使影像對位更具有彈性，符合對位的需求。

A Software System Developed Based on the Radial-Basis-Functions and Its Applications to Biomedical Images

Student: Yen-Chuen Huang Advisor: Yu-Tai Ching

Institute of Biomedical Engineering

National Chiao Tung University

ABSTRACT

In order to process biomedical images and make images register appropriately for the follow-up researches, we developed a GUI (graphic user interface) warping system and an algorithm based on the Radial Basis Function (RBF) is implemented. The algorithm adopting RBFs achieves local deformation and cooperates with the global polynomial function makes the registration more flexible. According to the prior experiences and knowledge, we select specific control-points or landmarks on both images to decide the non-rigid transformation in the system. We can then warp from one image to another efficiently.

誌　謝

首先誠摯的感謝指導教授荊宇泰博士，老師細心的教導使我得以一窺生醫影像處理領域的深奧，不時地討論並指點我正確的方向，使我在這些年中獲益匪淺，老師對學問的嚴謹更是我輩學習的典範。也感謝口試委員胡宇光教授、楊裕雄教授對論文與研究提供許多寶貴的建議，使得論文更加完善。

兩年裡的日子，實驗室裡共同的生活點滴，學術上的討論、言不及義的閒扯、讓人又愛又怕的宵夜、趕作業的革命情感、因為睡太晚而遮遮掩掩閃進實驗室.....，感謝眾位學長姐、同學、學弟妹的共同砥礪，你們的陪伴讓兩年的研究生活變得絢麗多彩。

感謝秉璋、昌杰學長們不厭其煩的指出我研究中的缺失，且總能在我迷惘時為我解惑，也感謝宗澤、志文、耿郁同學的幫忙，恭喜我們順利走過這兩年。

女朋友在背後的默默支持更是我前進的動力，沒有的體諒、包容，相信這兩年的生活將是很不一樣的光景。

最後，謹以此文獻給我摯愛的雙親。

Contents

List of Figures

Chapter 1
Introduction

In this thesis, we present an image warping software system developed based on Radial Basis Function (RBF) deformation. We show that the software system can be applied to biomedical images processing. Through the interactive interface, users can obtain the desired result for the follow-up researches or applications.

In the biomedical images analysis, it is a frequent demand for comparing images for analysis and diagnostic purposes. In order to achieve an efficient comparison, the images first need to be aligned. For example, medical diagnosis often benefits from the complementary information in images of different modalities. In order to fuse the complementary information, the alignment of the images is the first step to be performed to overcome the complication of displacement or deformation caused by patient motion and physical change.

Registration following by deformation is called warping. Warping has been studied for a long time. Bookstein [1] introduced thin-plate splines for medical image registration. Others investigated methods using RBFs for registration, such as Gaussian [2], multiquadrics [3], inverse multiquadrics [4]. By these RBFs, Wirth proposed point-to- point registration method on non-rigid medical images deformation [5]. A polynomial based RBF with compact support was first introduced by Wendland [6]. It has been used to model elastic registration of medical images [7]. Locally constrained deformation is another polynomial based RBF produce better results [8]. Moreover, the criteria to evaluate the accuracy of transformation functions of image registration are also proposed [9].

In this these, we show two examples that the proposed system can be applied. One is the reconstruct an aligned data from a stack of electron microscopic images. The other is an application to analysis of 2D gel electrophoresis images.

Usually, electron microscopic images have to be registered before follow-up manipulations. Electron microscope allows the investigation of the 3D structure of biological specimens, which is important to understanding their function. However, before the 3D reconstruction procedure, the images taken from the microscope have to be properly registered. One of alignment method is based on the minimization of an error function by means of inefficient exhaustive search procedures [10]. Redondo used a stochastic optimization approach to cope with this problem [11].

Recently, proteomics research has become a large growth area in the biosciences. Often, studies involve differential analysis of 2-D gel electrophoresis. Images acquired from 2-D gel electrophoresis experiments are also one of the applications for image registration. Mike Rogers [12] presents a robust and accurate 2-DE gel alignment algorithm which combines point matching and local image-based refinement. Kaczmarek [13] proposed a method of 2D gel image matching is based on fuzzy alignment of features. Software for the analysis of 2D gel images in the high throughput laboratories has been developed by Sorzano [14].

The structure of this thesis is described as follow. The first chapter gives the motivation and an introduction to relevant researches. In chapter 2, we describe the background material used in image registration tool. The detail of registration flowchart and our algorithm are reported in chapter 3. In addition, we introduce the environment of software development and test some examples by our system. The major experimental results of our system for biomedical images are demonstrated in chapter 4. Conclusion and future work are listed in chapter 5.

Chapter 2
Background Materials

In this chapter, we briefly introduce of the relative research work of image registration. First, in section 2.1 we report the foundation of image registration algorithm and introduce biomedical images.

In section 2.2, we describe one of the image registration methods, including the concept and the application to image registration in detail.

2.1. Image Registration

2.1.1 Definition of Registration

Image registration is a process to find the best alignment of two images. Registration following by deformation is called warping. The registration or warping defines a transformation that the points in one image are transformed to the points of another image so that two images are aligned in the spatial domain.

An image transformation is called *rigid* when only translations and rotations are allowed. If the transformation maps parallel lines onto parallel lines it is called *affine*. If it maps lines onto curves, it is called *elastic* or *non-rigid*. A transformation is called *global* if it applies to the entire image, and *local* if subsections of the image each have their own transformations defined.

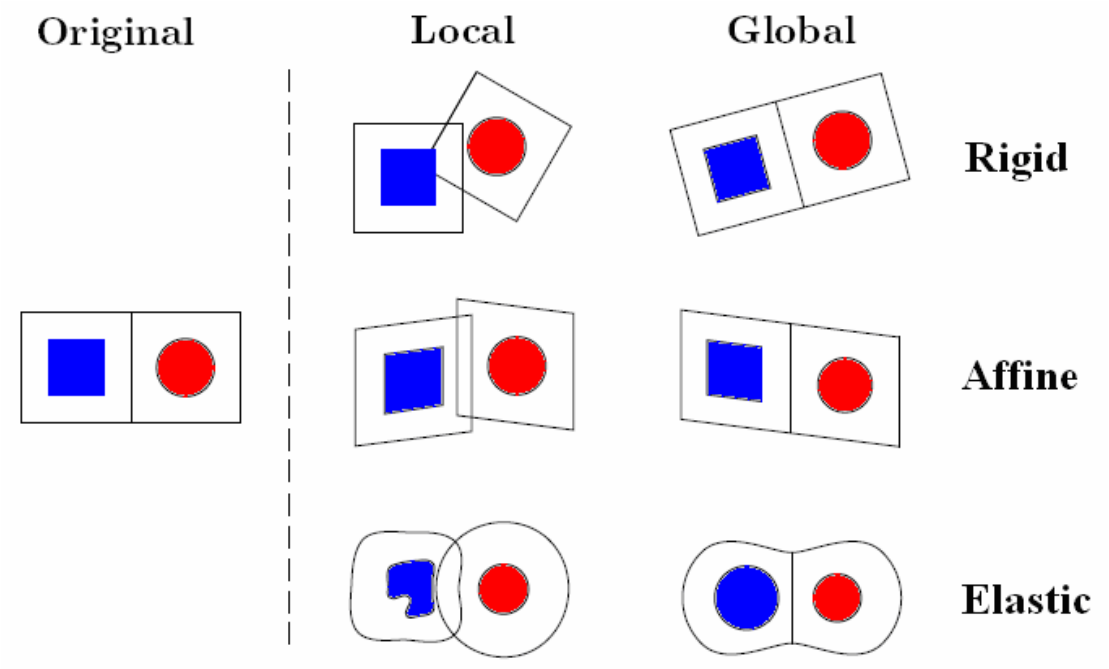

Fig. 2-1: The definition of registration

2.1.2 Biomedical Image Registration

Medical imaging provides insights into the size, shape, and spatial relationships among anatomical structures. For instance, computer-assisted tomography (CT) is very useful for imaging bony structures and dense tissue, whereas magnetic resonance imaging (MRI) and ultrasound (US) provide views of soft tissues. Additionally, functional imaging is becoming increasingly important both clinically and in medical research. For example, positron emission tomography (PET) and single-photon computed tomography (SPECT) imaging provide information on blood flow and metabolic processes. Very often, areas of the body are imaged with different modalities.

Biological images range from the visualization of ions, molecules, cells and tissues to the full size animals. Since the discovery of the electron microscope, imaging has been an important method in modern bioscience and its significance has grown tremendously.

Biomedical image registration often additionally involves elastic or non-rigid registration to cope with deformation of the subject which is due to breathing, anatomical changes, and so on. It generally refers to the process of identifying and subsequently aligning corresponding structures or objects from two biomedical images. To register two images, correspondence and a transformation must be found so that each location in source image can be mapped to a new location in the target image. This mapping should optimally align the two images wherein the optimality criterion itself depends on the actual structures or objects in the two images that are required to be matched.

We select the radial basis functions method to model our non-rigid transformation system, because it possesses some special properties and is easy for us to achieve the aim. We illustrate the reason as the following.

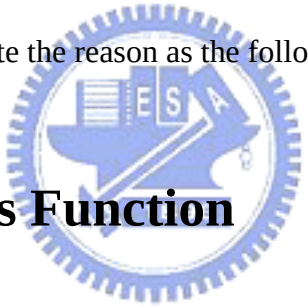

2.2. Radial Basis Function

A radial basis function (RBF) is a real-valued function whose value depends only on the distance from the origin, so that $\varphi(x) = \varphi(\|x\|)$ or alternatively on the distance from some other point c, so that $\varphi(x, c) = \varphi(\|x - c\|)$. Any function that satisfies the property $\varphi(x) = \varphi(\|x\|)$ is a radial basis function. The norm is usually Euclidean distance, although other distance functions are also possible.

Radial basis functions are typically used to build up function approximations of the form

$$y(x) = \sum_{i=1}^{N} w_i \varphi(\|x - c_i\|) \qquad (2.1)$$

where the approximating function $y(x)$ is represented as a sum of N radial basis functions, each associated with a different center c_i, and weighted by an appropriate coefficient w_i.

2.2.1 Selection of Radial Basis Function

Commonly used types of radial basis functions include $r = \|x - c_i\|$ and the following.

- *Gaussian:* $\varphi_G(r) = e^{-r^2/2\sigma^2}$,
- *Multiquadrics:* $\varphi_M(r) = (r^2 + c^2)^{1/2}$,
- *Inverse Multiquadrics:* $\varphi_{IM}(r) = (r^2 + c^2)^{-1/2}$,
- *Thin plate spline:* $\varphi_{TPS}(r) = r^2 \ln(r)$,
- *LCD:* $\varphi_{LCD}(r) = (1 - r^2)^3$,
- *Wendland:* $\varphi(r) = \begin{cases} p(r) & 0 \le r \le 1 \\ 0 & r > 1 \end{cases}$ where $p(r)$ is a specific polynomial,

The radial basis functions can be broadly divided into two types, global and local. The global functions influence the whole image. This type of functions is useful when registration process needs deformation of complete image in nature, such as the first four functions above. In these functions, location of each pixel is effected by each landmark which is computationally time-consuming and lacking of locality.

The choice of the type of RBF is crucial for the overall characteristics, such as the smoothness of the transformation function. We adopt Wendland functions as our radial basis functions. The common instances of Wendland functions are

$$\varphi_{3,0}(r) = (1-r)^2_+$$

$$\varphi_{3,1}(r) = (1-r)^4_+ \cdot (4r+1)$$

$$\text{where} \quad (1-r)^\nu_+ = \begin{cases} (1-r)^\nu & 0 \le r \le 1 \\ 0 & r > 1 \end{cases}$$

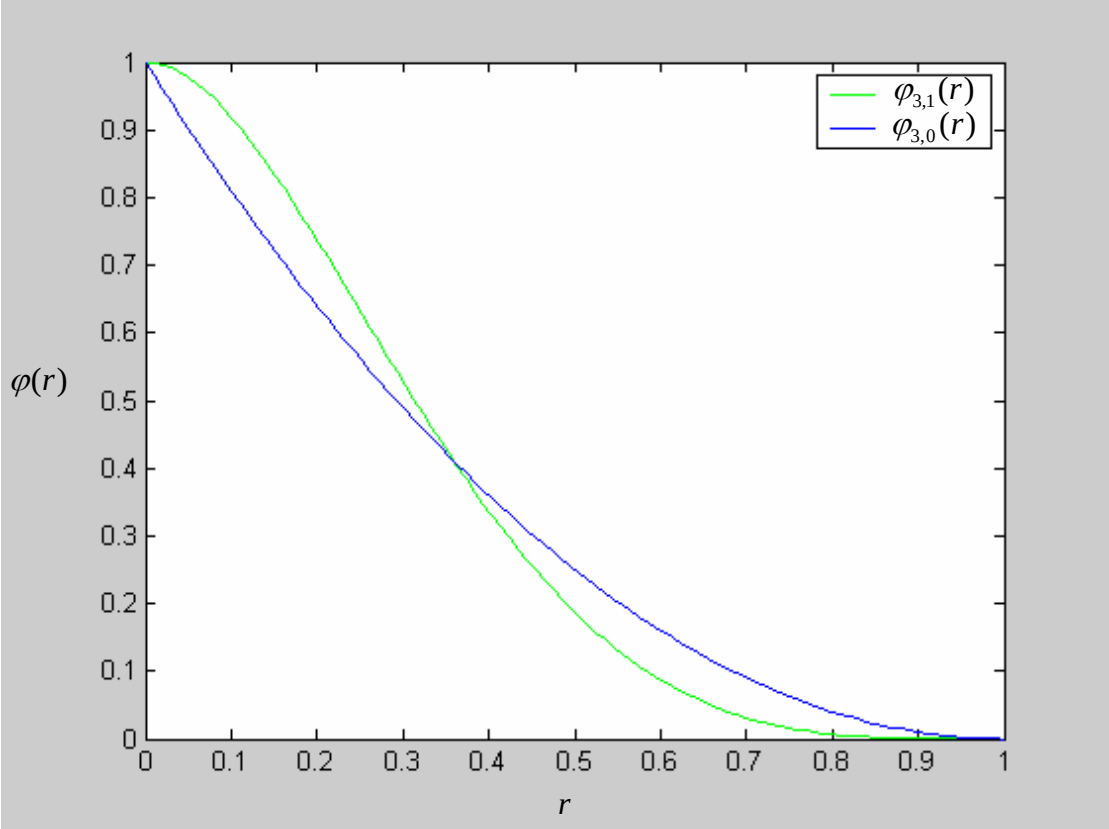

Fig. 2-2: Examples of Wendland functions used for local deformation

Locality. The mathematical properties of Wendland RBFs also hold for different a, such that $\varphi(r/a)$ has the locality parameter a, called *compact support*, which allows us to control their range of influence on the registration result and reach elastic registration.

Solvability. One of the advantages that we use Wendland RBFs is the solvability. In Wendland RBFs, the matrix involved is positive definite.

Efficiency. For efficiently solving the system, the computation is reduced as possible as we can by making the matrix sparse, especially for large datasets such as 3D images. In Wendland RBFs, the matrix involved is usually sparse.

2.2.2 Radial Basis Functions for Deformation

An RBF spatial transformation in d dimensions, denoted $T(\vec{x})$, $x \in R^d$, composed of $k = 1,...,d$ mapping functions, such that

$$T(\vec{x}) = [\, f_1(\vec{x}),..., f_k(\vec{x}),..., f_d(\vec{x})].$$

With RBFs, each of the mapping functions can be decomposed into a global component and a local component. This decomposition enables a family of transformations to be defined where the influence of each control point can be determined. Given n pairs of corresponding control points or landmarks, each of the k mapping functions of the RBF is in the following form:

$$f_k(\vec{x}) = P_{mk}(\vec{x}) + \sum_{i=1}^{n} w_{ik}\, g(r_i) \qquad (2.2)$$

where $P_{mk}(\vec{x})$ is a polynomial of degree m. For the RBF dealt with here, a linear polynomial ($m = 1$), i.e.,

$$P_{mk}(\vec{x}) = a_0 + a_1 x + a_2 y \quad (d = 2) \qquad (2.3)$$

is used. This makes the global component an affine transformation. $g(r_i)$ is a weighted elastic basis function, and r_i denotes the Euclidean norm defined by

$$r_i = \left\| \vec{x} - \vec{x}_i \right\|$$

between a point $\vec{x} = (x, y)$ and the control-point $\vec{x}_i = (x_i, y_i)$ in the source image (2-dimensional image), and w_i corresponds to the weight parameter. In order to use a RBF transformation, three or more non-collinear points must be specified.

The control-points of source image are decided by users, and in the meantime users choose the corresponding points of these control-points in the target image. The coordinates of these points are determined. Assume $f_k(\vec{x}_j) = u_{jk}$, $j = 1,2...,n$, where $\vec{x}_j$ is the j^{th} control-point of source image and u_j is corresponding point in the target image, then

$$f_x(\vec{x}) = a_0 + a_1 x + a_2 y + \sum_{i=1}^{n} w_i g(r_{ij}) \tag{2.4}$$

where $r_{ij} = \left\| \vec{x}_j - \vec{x}_i \right\|$ is the radial distance between respective control-points (x_i, y_i) and (x_j, y_j) in the source image.

There are $(n+3)$ coefficients in Eq. (2.2) that we need to calculate for each dimension. This system is composed of the n equations in Eq. (2.4) together with the following additional constraints

$$\sum_{i=1}^{n} w_i = \sum_{i=1}^{n} w_i x_i = \sum_{i=1}^{n} w_i y_i = 0 \tag{2.5}$$

The matrix form in one of dimension becomes

$$\begin{bmatrix} g(r_{11}) & \cdots & g(r_{1n}) & 1 & x_1 & y_1 \\ \vdots & \cdots & \vdots & \vdots & \vdots & \vdots \\ g(r_{n1}) & \cdots & g(r_{nn}) & 1 & x_n & y_n \\ 1 & \cdots & 1 & 0 & 0 & 0 \\ x_1 & \cdots & x_n & 0 & 0 & 0 \\ y_1 & \cdots & y_n & 0 & 0 & 0 \end{bmatrix}_k \begin{bmatrix} w_1 \\ \vdots \\ w_n \\ a_0 \\ a_1 \\ a_2 \end{bmatrix}_k = \begin{bmatrix} u_1 \\ \vdots \\ u_n \\ 0 \\ 0 \\ 0 \end{bmatrix}_k \tag{2.6}$$

where $w_1 \cdots w_n$ and a_0, a_1, a_2 are unknown and others are known.

After solving the linear functions above, all coefficients are obtained and substitute into Eq. (2.2) for all the other points in the source image. If landmarks with zero displacement, i.e. which is the case if the source landmark $\vec{x}_j$ and the target landmark u_j coincide, can be used to fix the transformation at these points.

Chapter 3
Overview of the Proposed Method

In this chapter, we describe each part of our image registration system, including the flow chart and the algorithms. We specify every step in the implementation and something should be noticed in the processing of image registration. At last, we apply our method to a phantom image of grid and a picture familiar with people to test the performance.

3.1. Image Registration with Wendland RBFs

3.1.1 The Flow Chart and Algorithm

Although the thesis focuses on local non-rigid registration together with global transformation, we still should pay attention to the topology of points in the image. Fornefett [7] calculated the necessary conditions for the Jacobian matrix in 2D images to be positive in case of isolated landmark and obtained the following result.

$\varphi_{3,1}(r/a)$	$\varphi_{3,2}(r/a)$	$\varphi_{LCD}(r/a)$	$\varphi_G(r)$
$a > 2.98\Delta$	$a > 3.54\Delta$	$a > 2.43\Delta$	$\sigma > 0.86\Delta$

Fig. 3-1: The restriction of compact support

$\Delta = \max(\Delta_1, \Delta_2)$, where Δ_1 and Δ_2 are the displacements from the source landmark to corresponding target landmark in x and y coordinate.

Obviously, when the displacement of one landmark between the source image

and target image is large, it means that one point of the source image needs to deform with a large-scale. Therefore, the registration has to utilize the large compact support to influence neighbor points. As one conclusion, we can say that the closer the landmarks are placed the smaller the locality parameter can be chosen.

Algorithm

1) Users select control-points in the source image and corresponding target image.

2) Calculate the Δ value.

3) Choose one of Wendland RBFs, such as $\varphi_{3,1}$, $\varphi_{3,2}$.

4) Calculate the range of compact support by Fig. 3-1 to keep the property of topology and users can decide the value in accordance with the range.

5) Solve the equation (2.6) and obtain the coefficients $w_1 \cdots w_n$ and a_0, a_1, a_2.

6) Use these coefficients in step 5 into Eq. (2.2), then all points of source image can be calculated corresponding locations after image registration.

7) Draw all corresponding locations and form the result image.

8) Check on the result image whether satisfies users' expectancy. If it is not, repeat step 1 with adding control-points and keep going to step 7, else done.

Now, according to the algorithm above we show the flow chart of our image registration steps as the following

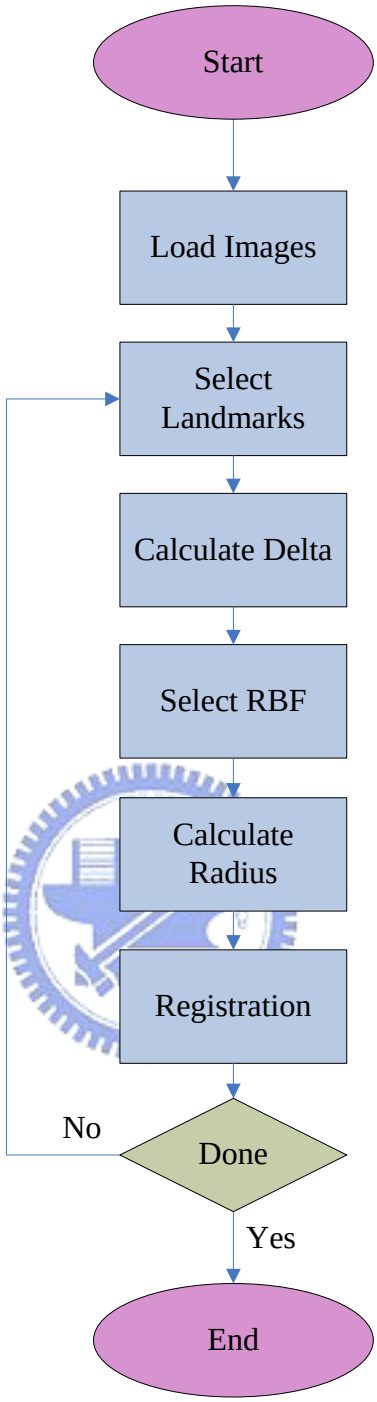

Fig. 3-2: The flowchart of our registration algorithm

3.1.2 Development of User Interface

The purpose of image registration obtains a desired alignment. Therefore, an interactive interface can be very helpful. Interactive methods reduce user bias by

performing certain key operations automatically while still relying on the user to guide the registration. According to this objective, we choose a windows development environment, named Qt.

There are several advantages of suing Qt over the other window programming system. First, Qt is free and open-source software. Besides, the worthiest thing we utilize Qt is that it is a cross-platform application development framework, widely used for the development of GUI programs, and also used for developing non-GUI programs such as console tools and servers. Qt is most notably used in KDE, Google Earth, Skype, Adobe Photoshop Album, VirtualBox and OPIE. It is produced by Nokia's Qt Software division.

Qt uses C++ with several non-standard extensions implemented by an additional pre-processor that generates standard C++ code before compilation. It can also be used in several other programming languages. It runs on all major platforms, such as Widows, Linux, Mac…etc.

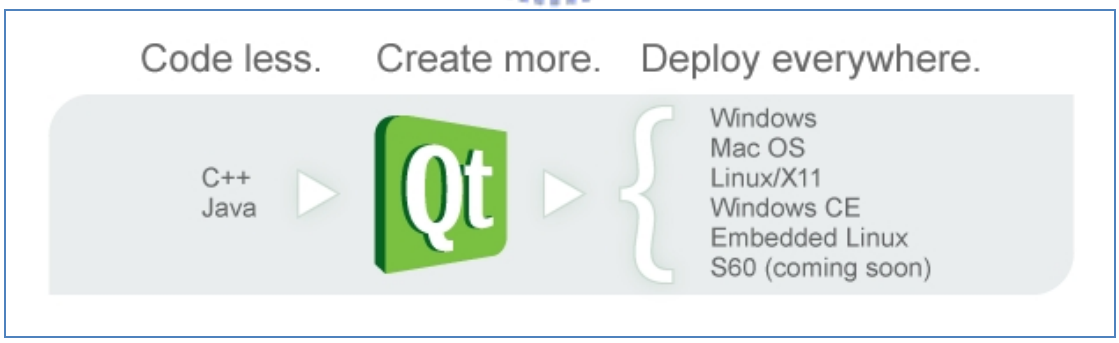

Fig. 3-3: The architecture of Qt environment

The design of interface window is separated by three parts. One is the operation of source image and the other is the operation of target image. The third part is the major steps of image registration in our algorithm.

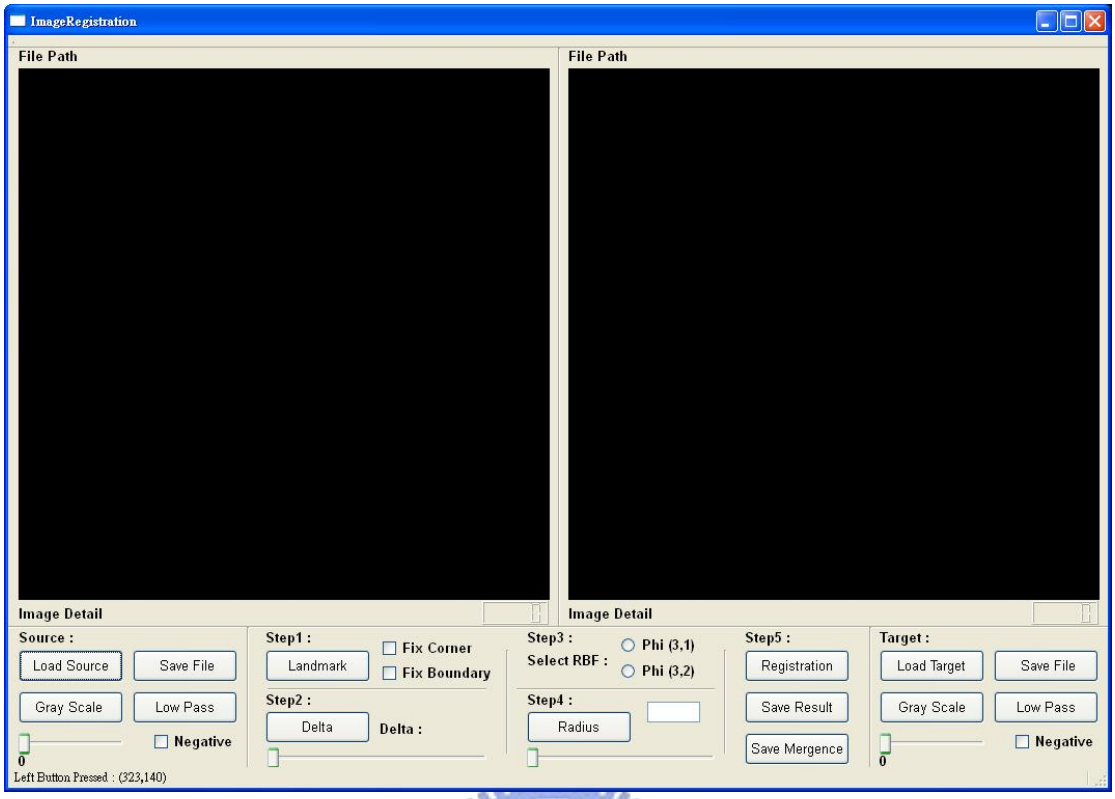

Fig. 3-4: The user interface of our registration

3.2. Examples of Our Image Registration

In order to test our registration algorithm and system, we apply the tool to a phantom image and a human face.

Firstly, we do the test in a phantom of grid. We attempt to test the locality of deformation, so the corners of images are fixed by 4-pair landmarks to avoid the global transformation. Next, we select 4 landmarks on the corner of the black square in the source image of phantom and the corresponding landmarks are selected on the grid line outside the black square in the target image. The purpose of control-points selection is to magnify the black square. The result is shown as Fig. 3-6.

We can observe the test result and find that it reaches the effect of local magnification. Simultaneously, there are 16 black spots keeping the shape and location. It means they are not influenced by our control-points selection.

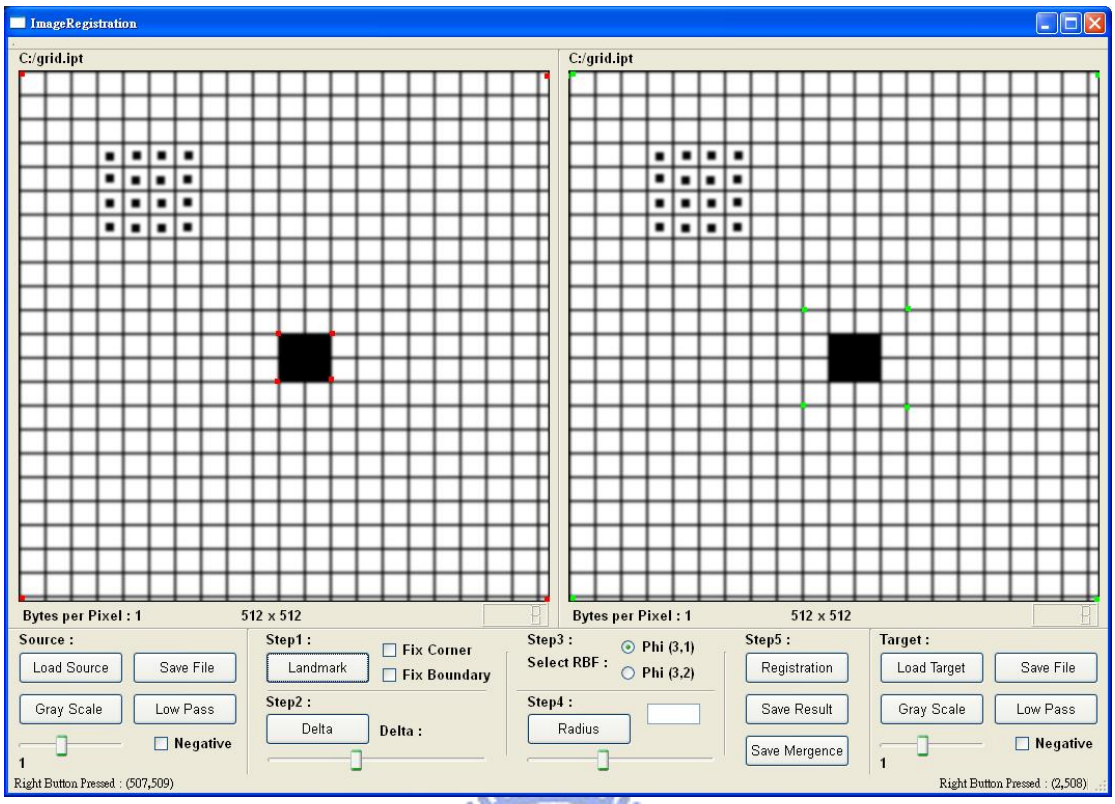

Fig. 3-5: The selection of landmarks in phantom image of grid

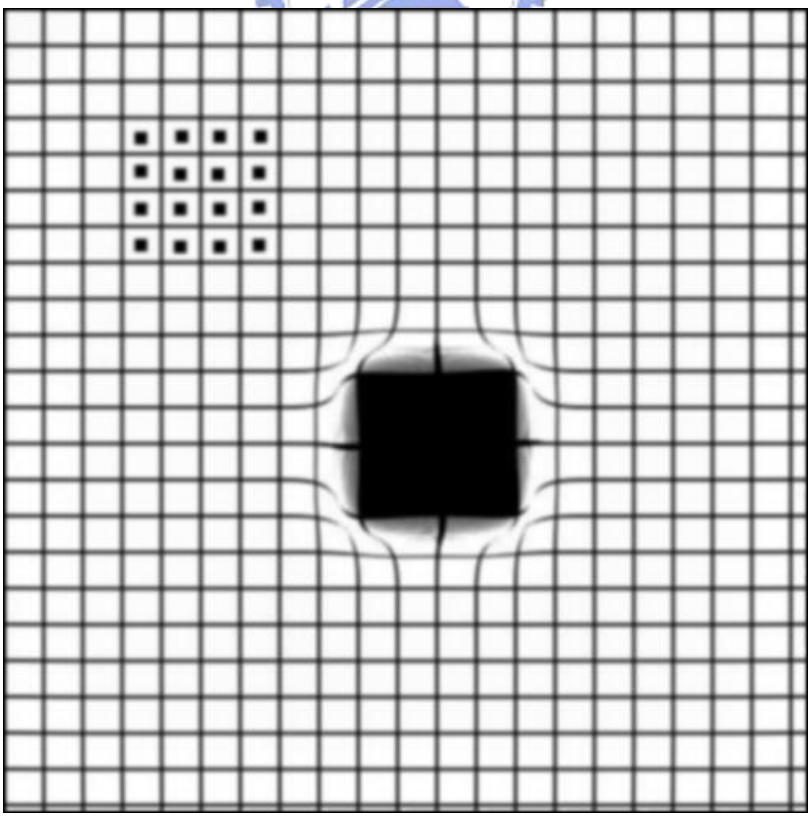

Fig. 3-6: The result of image registration from phantom image

Secondly, the famous picture, Mona Lisa, is manipulated and we observe the deformation result.

As the grid example, we fix the corners and there are another 4-pair landmarks selected. The choice of landmarks is for the reason that we want to make the world-famous smile become unhappy countenance.

Therefore, we select the 2 control-points on the end-point of mouth and 2 control-points for the restriction of RBF transformation mentioned in Chapter 2 (three or more non-collinear points must be specified).

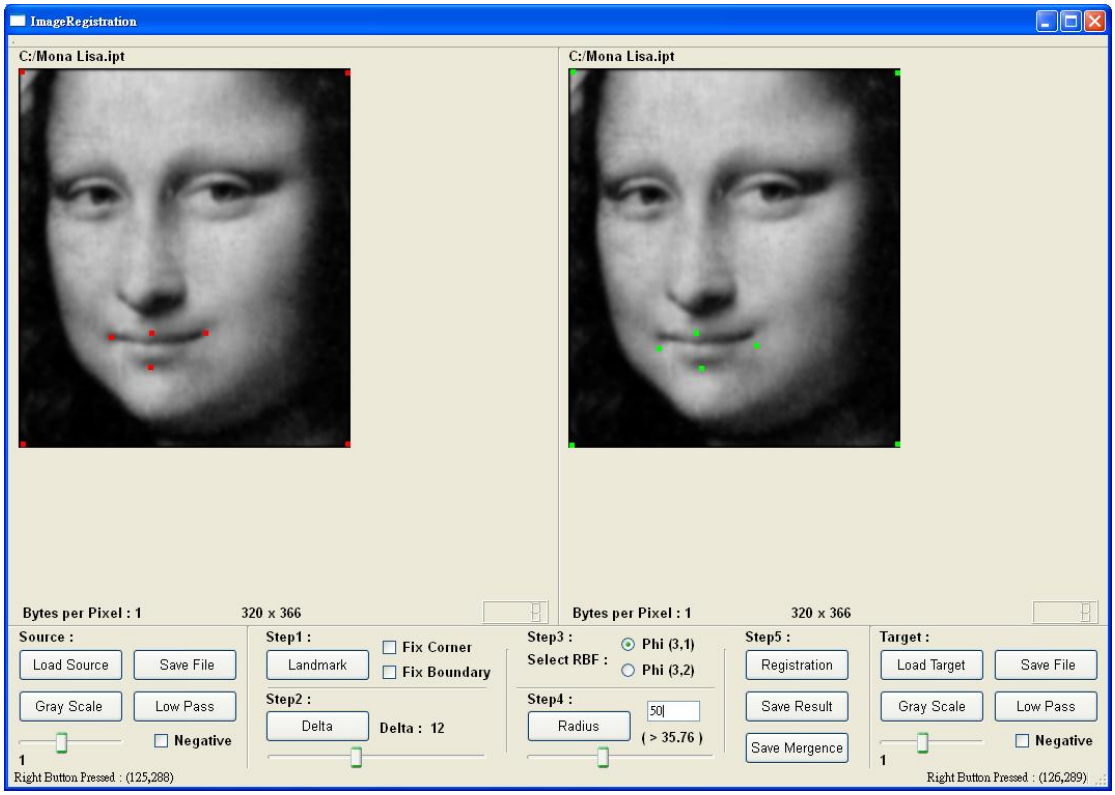

Fig. 3-7: The selection of landmarks in Mona Lisa picture

Fig. 3-8: The result of image registration from Mona Lisa picture

Observe on the result, the performance of registration is significant. Exception for the neighborhood of mouth, all points of the image are rarely deformed. At the same time, the deformation of mouth shows that Mona Lisa is in bad mood.

Chapter 4
Main Result

In this thesis, we execute the registration steps and apply the method to process electron microscopic images and 2-D gel electrophoresis images.

In section 4.1, we introduce the electron microscopic images and the problem which this kind of biological data confronts. Then, some results are presented by our image registration. 2D gel electrophoresis images are important biological data in proteomics. In section 4.2, 2D gel electrophoresis images are also experimented by our algorithm.

4.1. Image Registration of Electron Microscopic Images

Electron microscopes are dynamic rather than static in their operation, requiring extremely stable high-voltage supplies and stable currents. As they are very sensitive to vibration and external magnetic fields, electron microscopes must be located in stable buildings with special services such as magnetic field canceling systems for achieving high resolutions.

The combination of information from different electron microscopic images (EM) taken with the specimen at different slices is crucial to 3D reconstruction. Usually, when the experimenter deals with the sample, such as tissue, it can not be avoided invasive operations to produce biopsy specimen. Therefore, in practice EM images could be severely corrupted by noise, deformations and other measurement errors

which turn the alignment or registration into a problem. An essential step before the reconstruction is a proper registration so that the images are oriented appropriately.

Now, we register 6 slices (Fig.4-1) of EM data from biological experiments by using our system. Firstly, we select the No. 60 slice as the standard. Then, No. 61 ~ No. 65 are the source images waiting for registration where successive numbers mean adjacent slices. The experiment processes are as following.

1) Set No. 61 slice as source image and No. 60 as the target image. The result of registration from No. 61 to No. 60 names R61. (Fig.4-2 ~ Fig.4-3)
2) Set No. 62 slice as source image and R61 as the target image. The result of registration from No. 62 to R61 names R62. (Fig.4-4 ~ Fig.4-5)
3) Set No. 63 slice as source image and R62 as the target image. The result of registration from No. 63 to R62 names R63. (Fig.4-6 ~ Fig.4-7)
4) Set No. 64 slice as source image and R63 as the target image. The result of registration from No. 64 to R63 names R64. (Fig.4-8 ~ Fig.4-9)
5) Set No. 65 slice as source image and R64 as the target image. The result of registration from No. 65 to R64 names R65. (Fig.4-10 ~ Fig.4-11)

In order to show the performance of our algorithm, we have to compare the result of image registration with the target image. Therefore, every step above also merges the result with the target in one image. Apply red color to result image and green color to target image. The mergence image shows the yellow color when two images have the same gray level value at certain point, else they represent the mixed color by the percentage of gray level.

This experiment show a noticeable result through 15 landmarks selected in registration (Fig.4-2 ~ Fig.4-11).

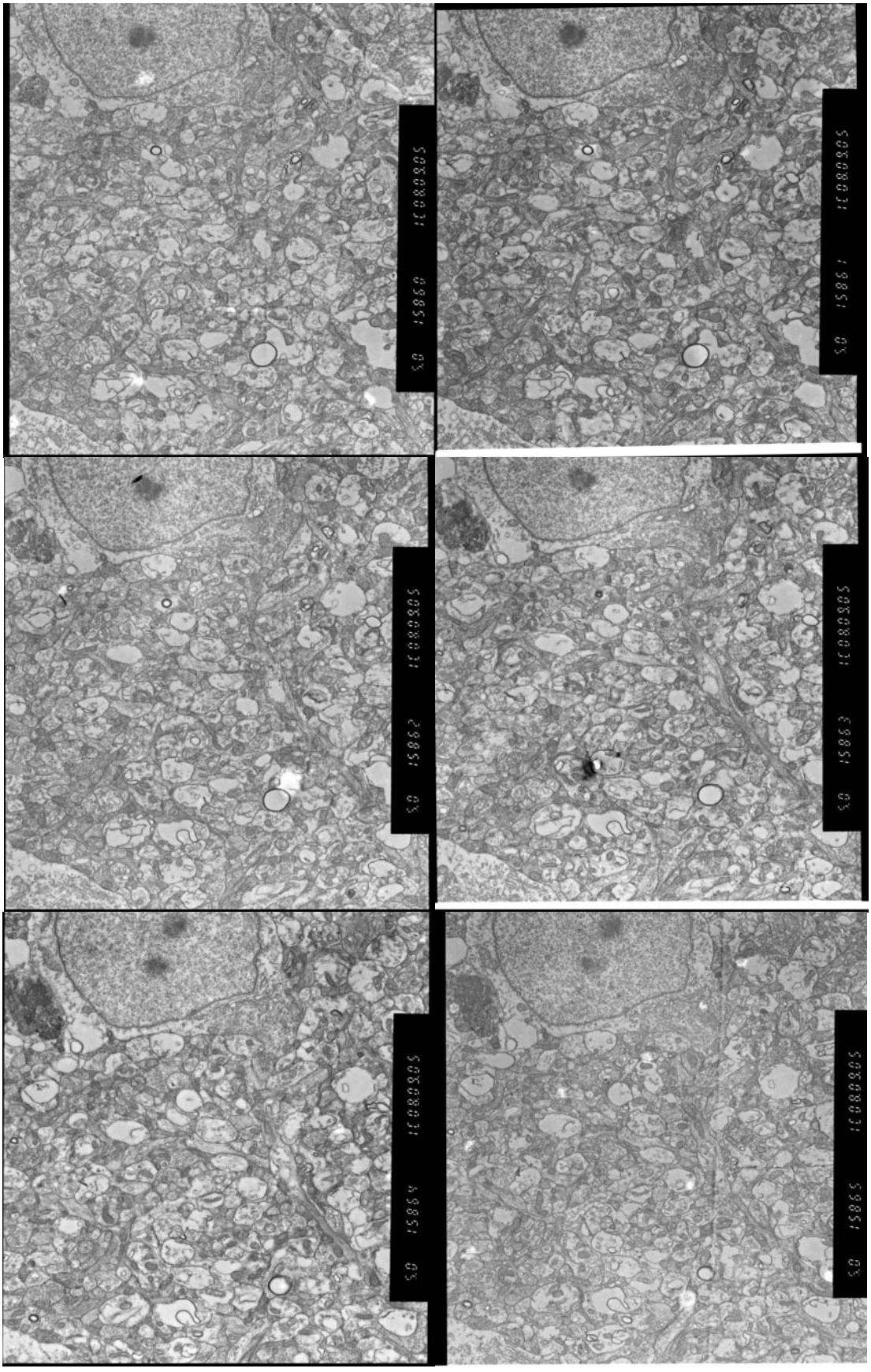

Fig. 4-1: No. 60 ~ No. 65 are EM images of successive tissue segments

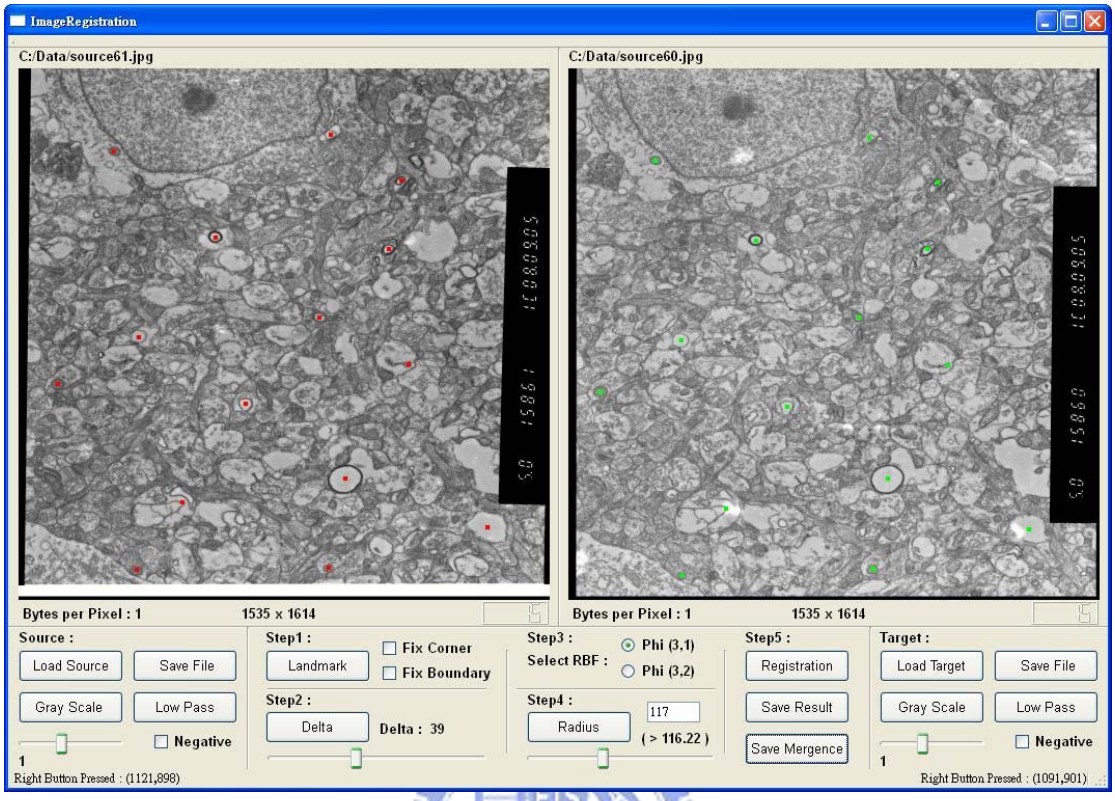

Fig. 4-2: Image registration from the source of No.61 to the standard (No.60)

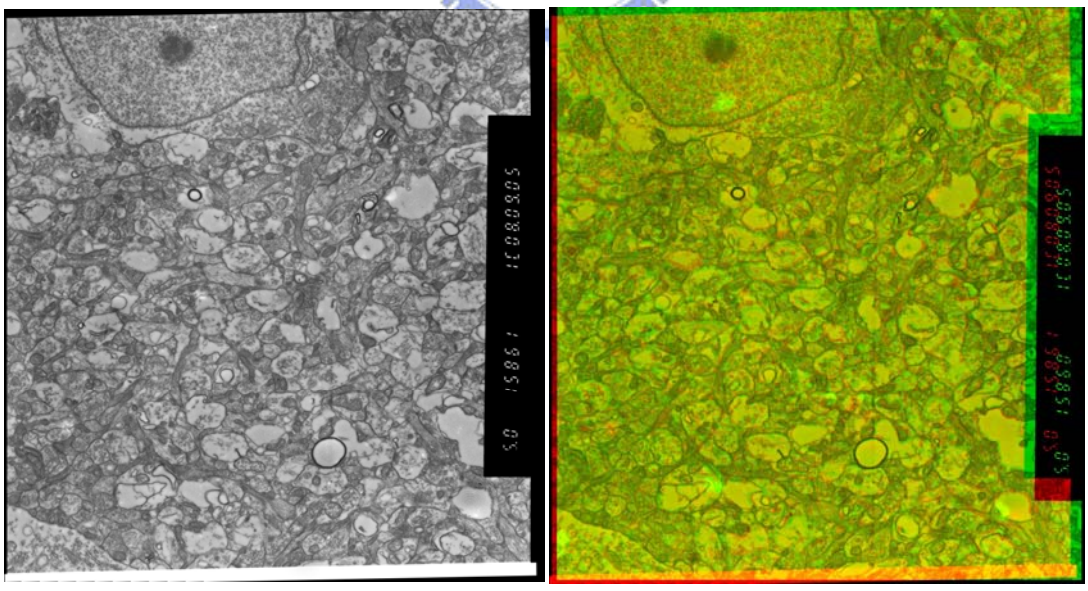

Fig. 4-3: The result of registration (R61); the mergence of R61 and No.60

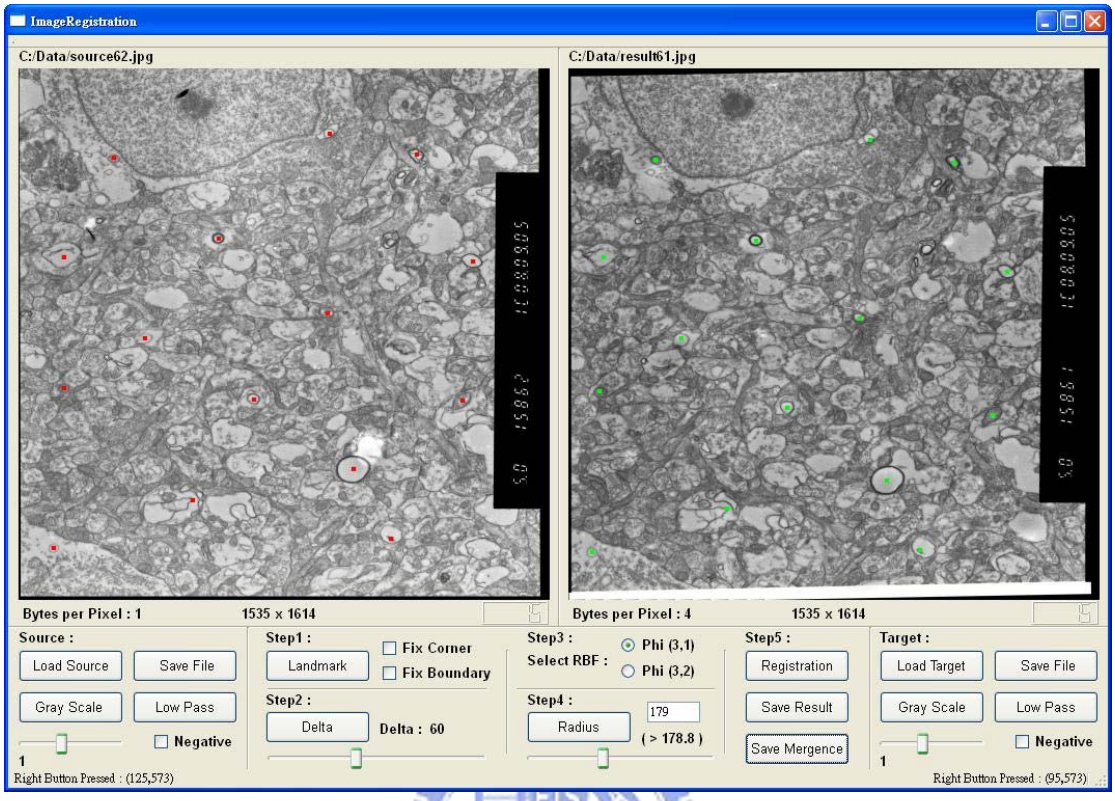

Fig. 4-4: Image registration from the source No.62 to the target R61

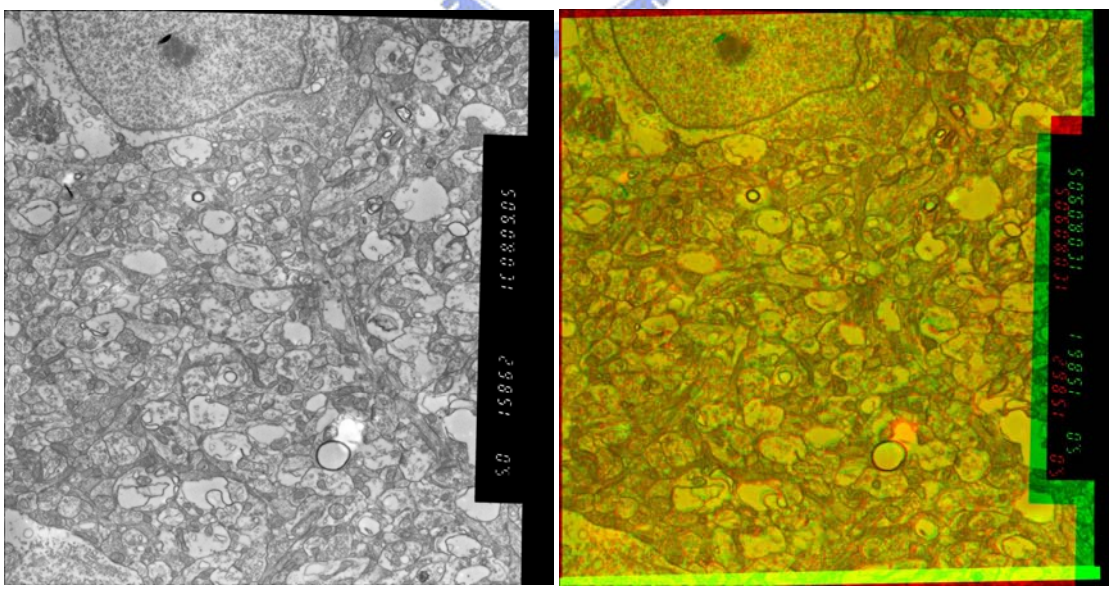

Fig. 4-5: The result of registration (R62); the mergence of R62 and No.61

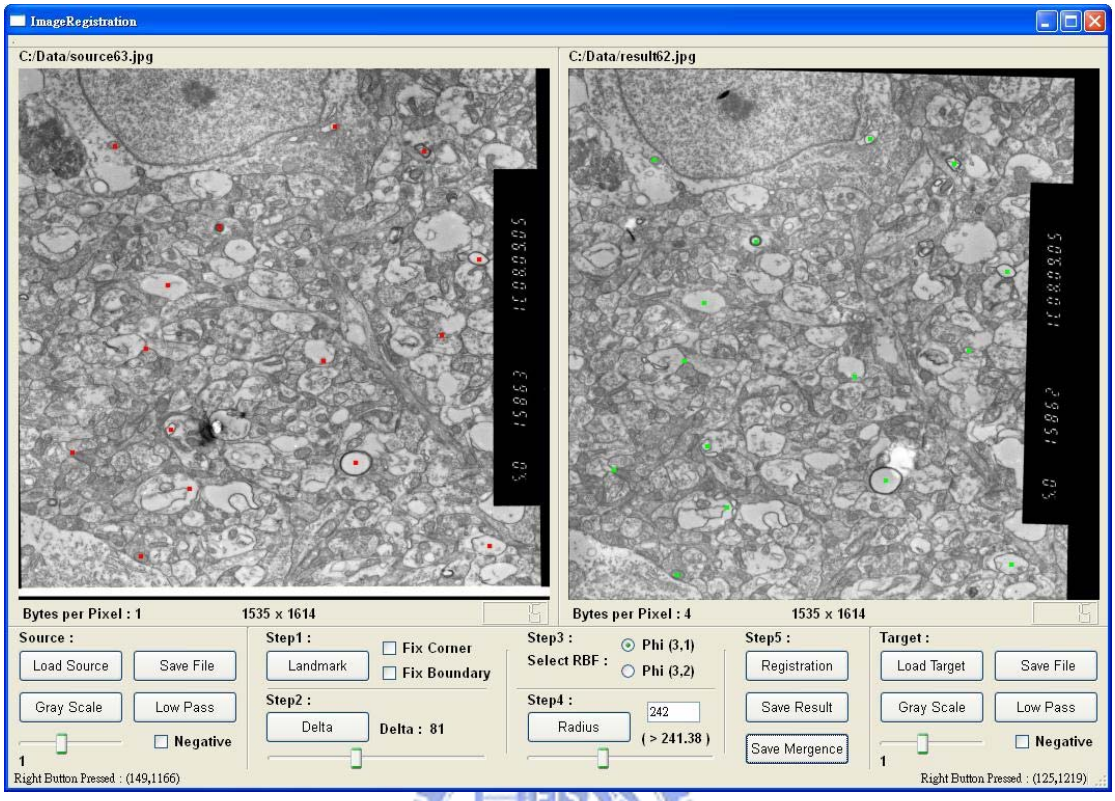

Fig. 4-6: Image registration from the source No.63 to the target R62

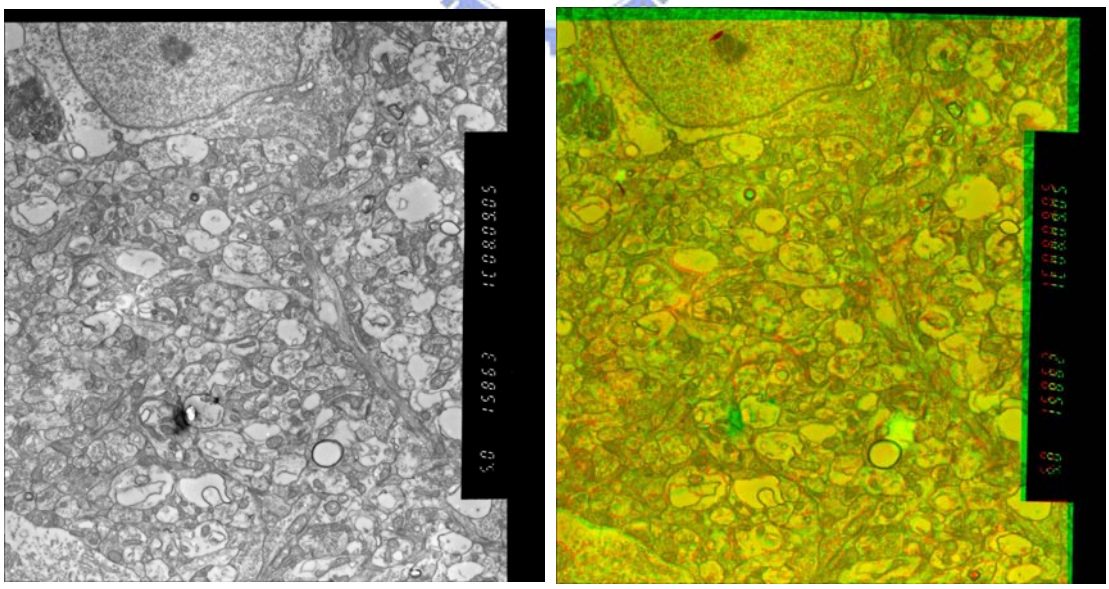

Fig. 4-7: The result of registration (R63); the mergence of R63 and No.62

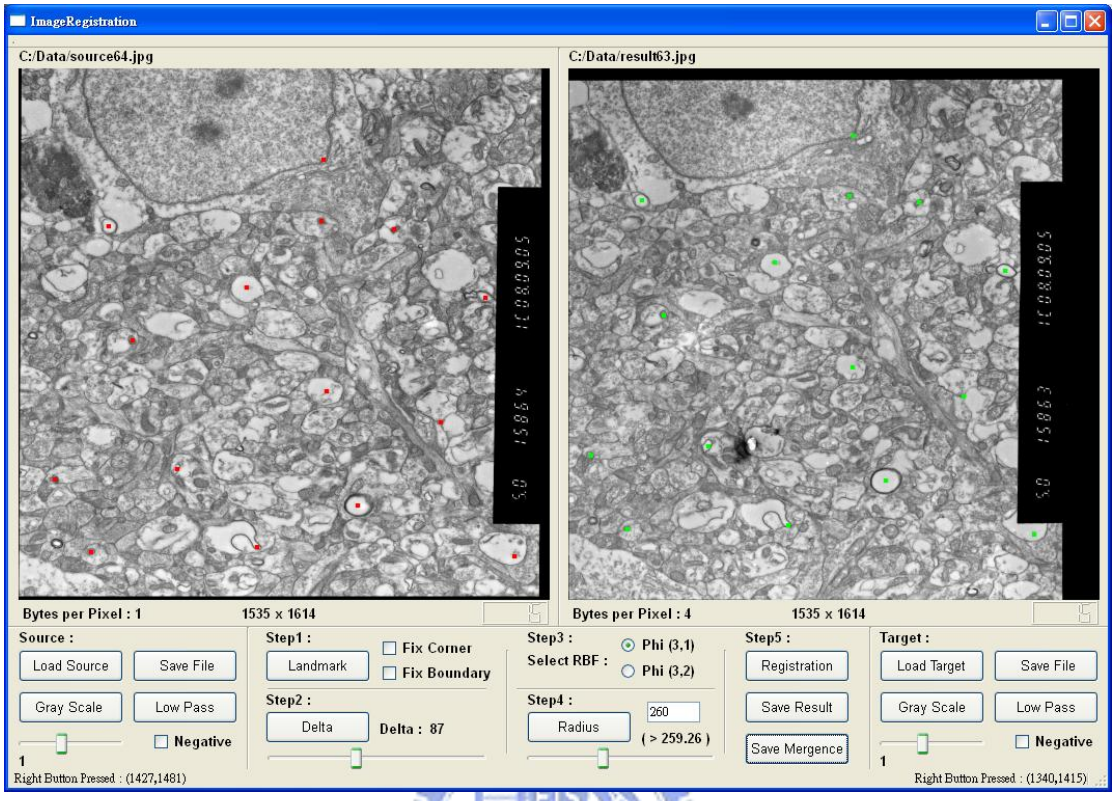

Fig. 4-8: Image registration from the source No.64 to the target R63

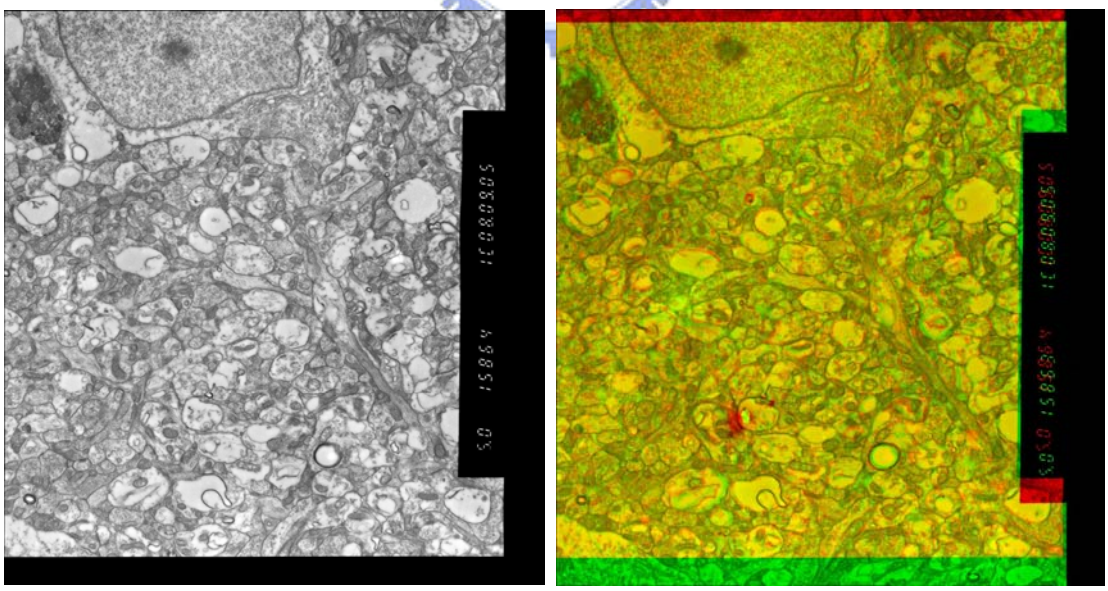

Fig. 4-9: The result of registration (R64); the mergence of R64 and No.63

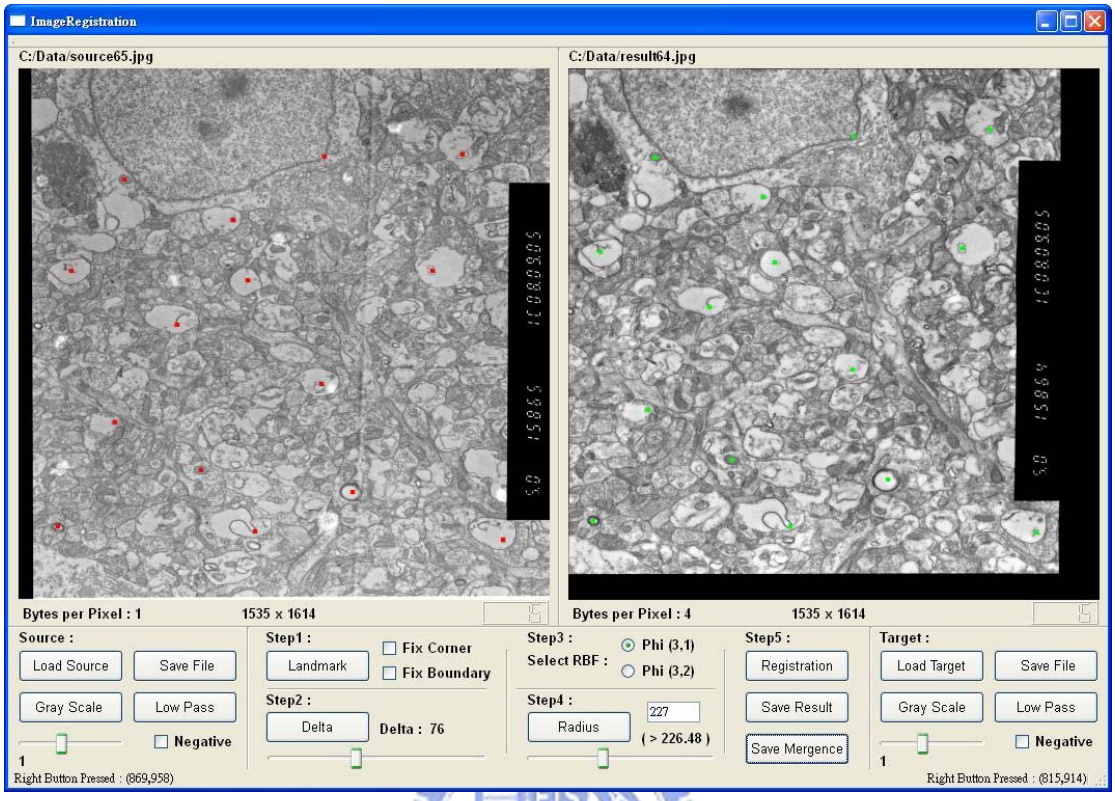

Fig. 4-10: Image registration from the source No.65 to the target R64

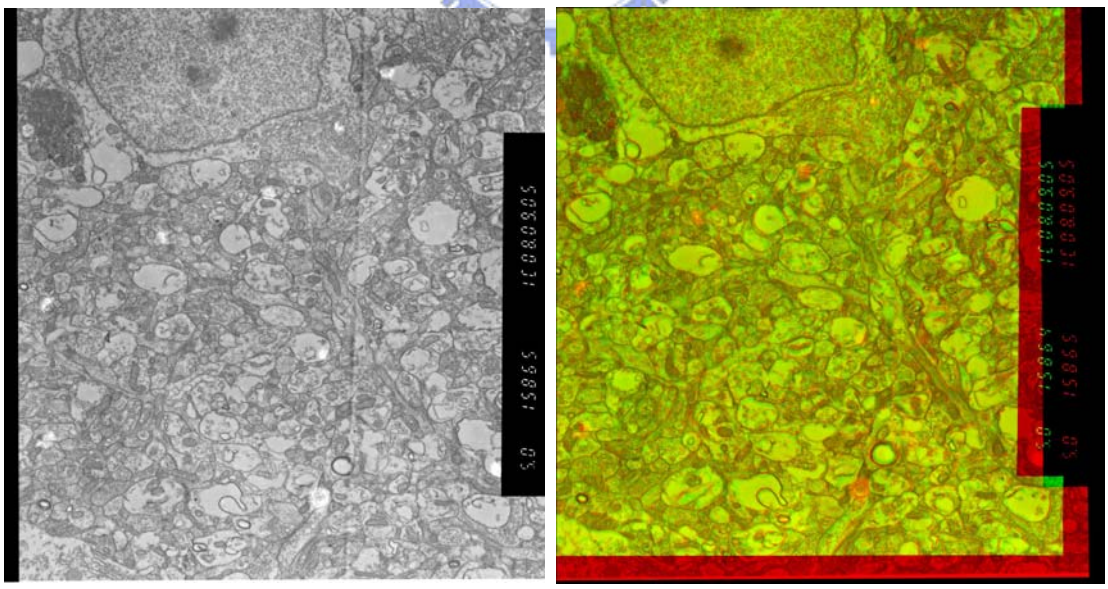

Fig. 4-11: The result of registration (R65); the mergence of R65 and No.64

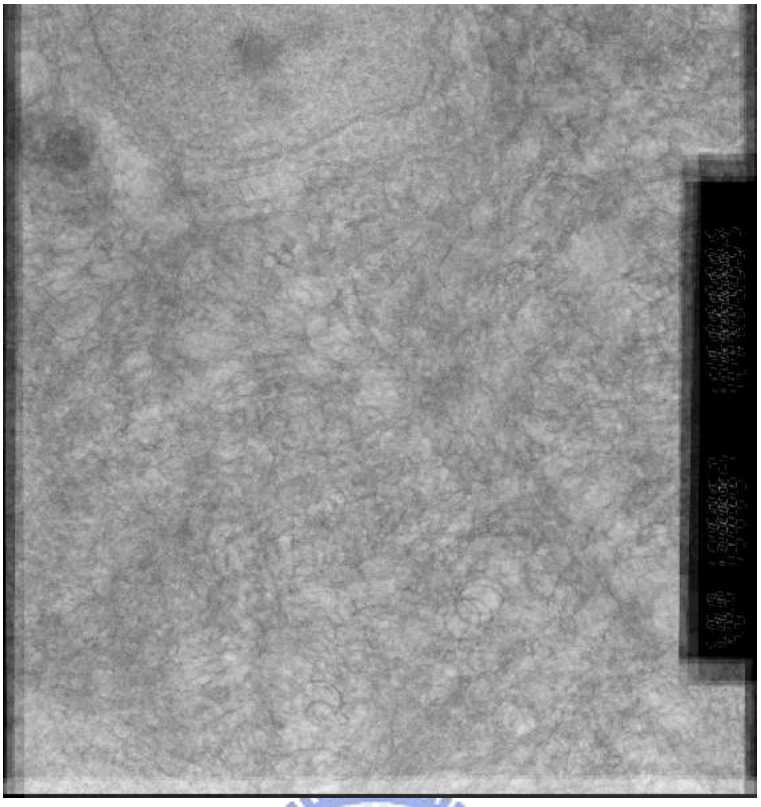

Fig. 4-12: The stack of 6-slice source EM images

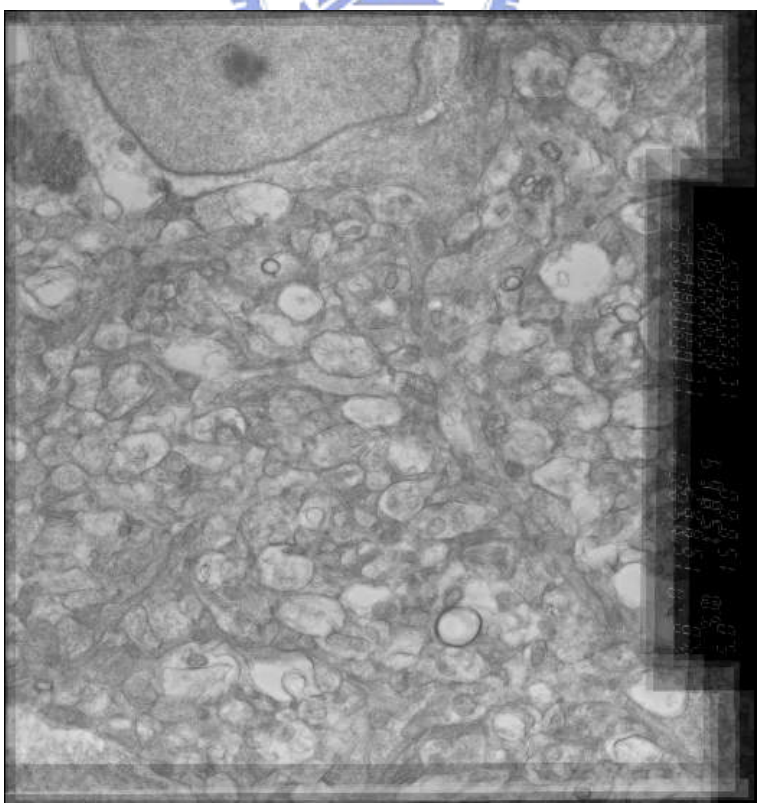

Fig. 4-13: The stack of 6-slice result EM images

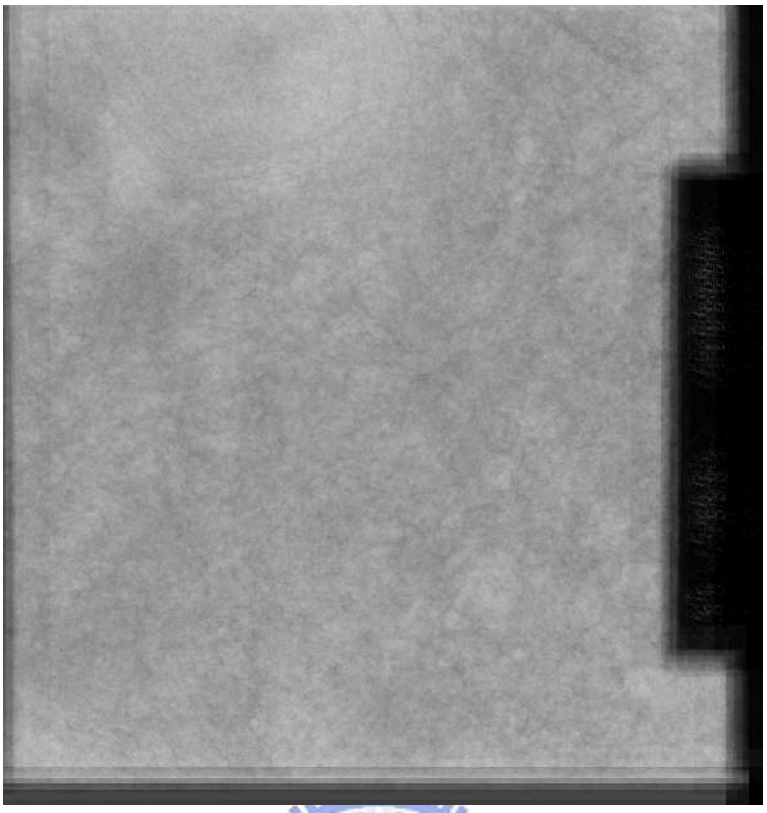

Fig. 4-14: The stack of 25-slice source EM images

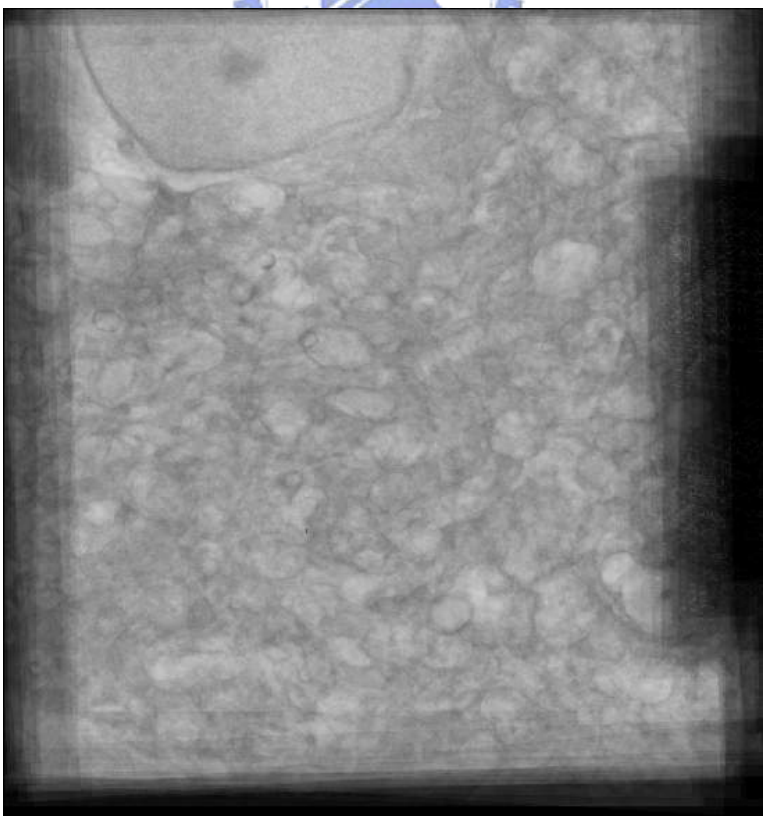

Fig. 4-15: The stack of 25-slice result EM images

After the experiment of 6-slice EM images, we put result images (Fig.4-2 ~ Fig.4-11) together in one image, and also manipulate source images (Fig.4-1). Obviously, Fig.4-12 reveals that the 6 successive slices of EM data do not orient well because the stack of them can not be found clear outline. However, the stack of result images (Fig. 4-13) can be observed the contours of cell.

Further, we experiment more successive slices of EM images and similarly put them together to a stack. When 25 slices of source EM images stack together, it is totally disordered (Fig.4-14). The result of 25-slice registration still sees the contour of the biggest cell in the upper image.

Besides, from EM data sometimes there is apparent global displacement between 2 adjacent slices, such as Fig.4-2. There is a black column in the right of result image (Fig.4-3 R61) and still achieves good registration result (Fig.4-3 the mergence image). This clarifies that our tool not only achieves local deformation but also gives consideration to global alignment between two images.

4.2. Image Registration of 2-D Gel Electrophoresis Images

In this section, we applied our registration algorithm to the registration of experimental 2- dimensional gel electrophoresis (2-DE) images (Fig.4-16).

2-DE is a procedure to separate and identify the proteins expressed by an organ, tissue, or cell, at a given time and under certain conditions. Proteins are separated in a perpendicular direction according to their mass by electrophoresis in gels, and these proteins will form spots after imaging.

To study protein expression in healthy and diseased tissues, many samples ought to be compared, to eliminate differences caused by individual diversity of the patients

and to identify proteins related to the disease. By comparing healthy and diseased tissues on the protein level, it is possible to identify the potential protein targets as diagnostic markers. Therefore, the analysis of 2-DE plays an important role in proteomics.

However, the spot position remarkably depends on experimental conditions, and can not be specified uniquely. In order to distinguish the influence of different conditions on proteins, image processing has to be done on experimental results.

In other words, we are interested to know which proteins are present in one gel and absent from the other or which certain spot in one gel becomes darker or lighter than the other. Establishment of registration between different 2-DE images will improve the accuracy of identification.

The same as section 4.1, the process produces the result of registration and the mergence of result and target image (Fig.4-17) by 10 landmarks selection.

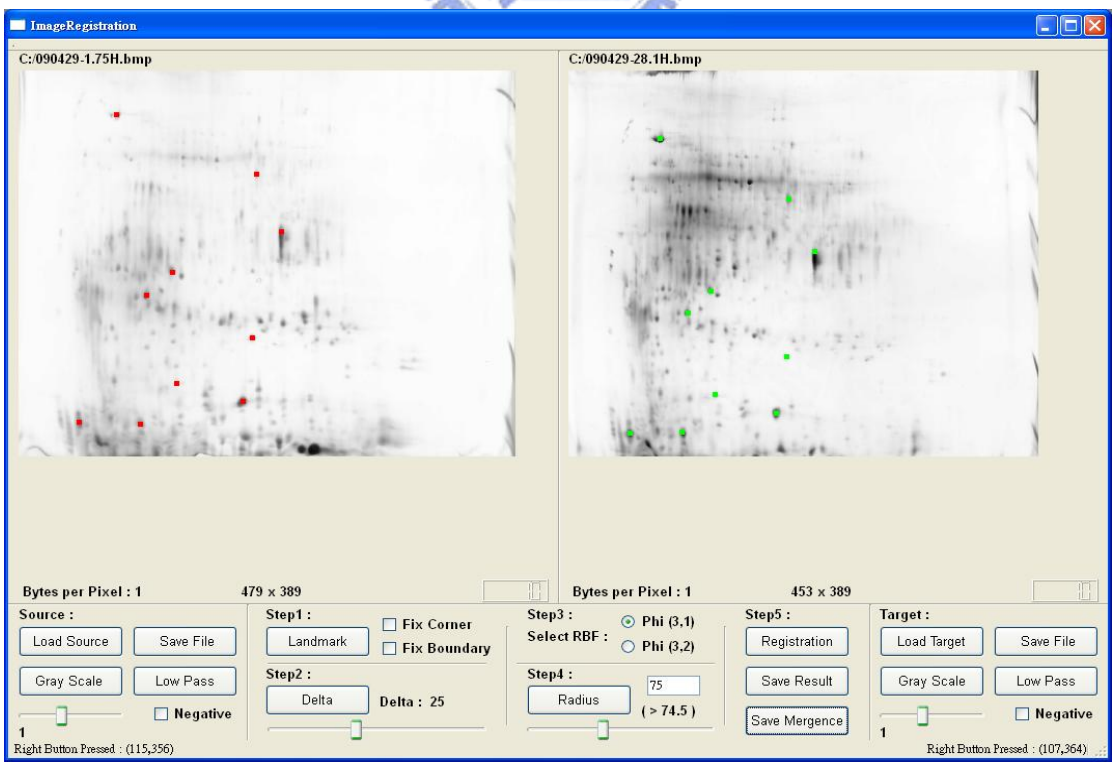

Fig. 4-16: Image registration from two different 2-DE images

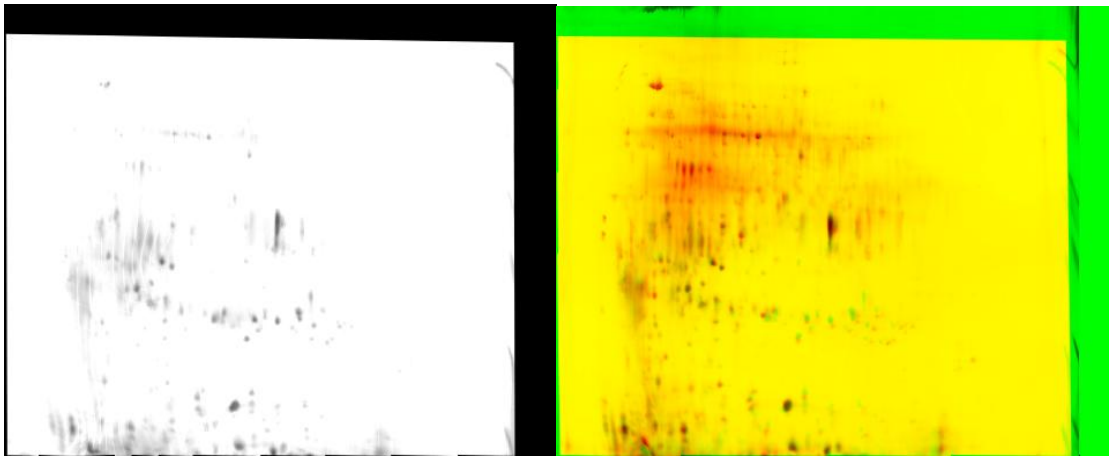

Fig. 4-17: The result of registration; the mergence of result and target

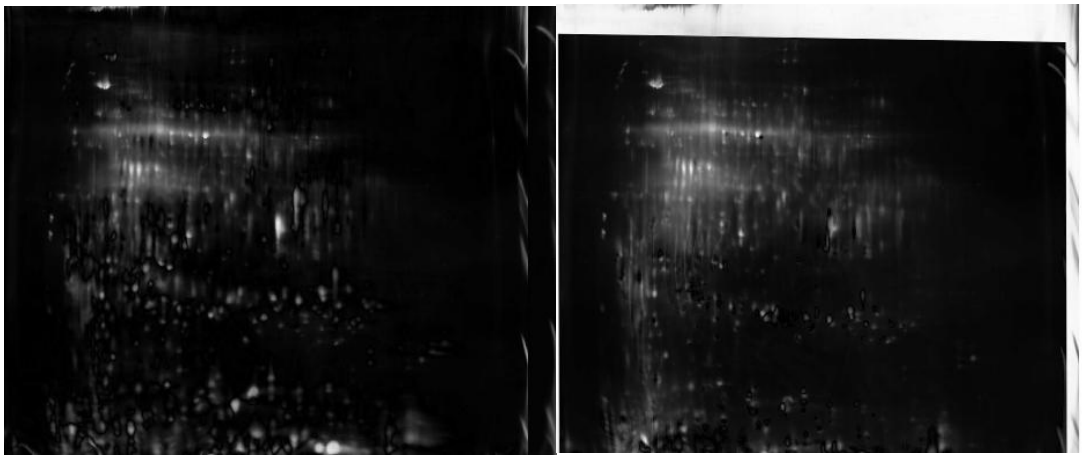

Fig. 4-18: Difference before registration; difference after registration

Moreover, we compare the difference (Fig.4-18 left) between the source and target image before registration. Then, we also calculate the difference (Fig.4-18 right) after registration.

In the Fig. 4-17, we can find some black spots and these are the same location which proteins move to in different biological conditions. Red spots or green spots mean that some proteins just appear in one of experimental conditions. By means of registration system, researcher can go a step further to analyze proteins.

Chapter 5
Conclusion and Future Work

In this thesis, we build a tool for image registration and warping with global and local deformation. Through our tests and experiments, Wendland radial basis functions with compact support can be very useful to cope with the local changes in an image and the global term in transformation equation is also suitable for biomedical images. However, usually the similarity measures should be judged the quality of registration by users or experts. It is worth researching an algorithm to evaluate the performance by impersonal data.

Although our system can provide interactive image registration with 2-dimension images, there are portion of 3-dimension data in biomedical images. Progressing to 3-dimension image registration is the next step we can make. Furthermore, such as EM data, we have accomplished a set of usable registration result. Next step, 3D structure reconstruction should be proceeded by computer graphics method in the future.

So far, control-points or landmarks selection is executed by users in our interactive interface. There are some advantages over this mode, such as precise selection by experts' experiences. It can lead to high performance of registration. Nevertheless, sometimes quantities of data need to be registered expeditiously. It does require automatic detection of landmarks instead of human eyes. In the future, the development of auto-searching for landmarks embedded in our system is very helpful.

Bibliography

[1] F.L. Bookstein, “Principal warps: thin-plate splines and the decomposition of deformations,” *IEEE Transactions on Pattern Analysis and Machine Intelligence*, 11 (6), 567–585, 1989.

[2] N. Arad, D. Reisfeld, “Image warping using few anchor points and radial functions,” *Computer Graphics Forum*, 14, (1), 35–46, 1995.

[3] J.A. Little, D.L.G. Hill, D.J. Hawkes, “Deformations incorporating rigid structures,” *Computer Vision and Image Understanding*, 66, (2), 223–232, 1997.

[4] D. Ruprecht, H. Mu¨ller, “Free form deformation with scattered data interpolation methods,” *Computing Supplementum*, 8, 267–281, 1993.

[5] M.A.Wirth, C. Choi, A. Jennings, “Point-to-point registration of non-rigid medical images using local elastic transformation methods,” *IPA97, Conference Publication* No.433 IEE, 1997.

[6] H. Wendland, “Piecewise polynomial, positive definite and compactly supported radial functions of minimal degree,” *Advances in Computational Mathematics*, 4 , 389–396, 1995.

[7] Fornefett M., Rohr K., Stiehl H.S., “Radial basis function with compact support for elastic registration of medical images,” *Image and Vision Computing*, 19, 87–96, 2001.

[8] Peng, W., Tong, R., Qian, G., Dong, J., “A local registration approach of medical images with niche genetic algorithm,” In *10th Internat. Conf. on Computer Supported Cooperative Work in Design*, pp. 1–6, May 2006.

[9] Adil Masood Siddiqui, Asif Masood, Muhammad Saleem, “A locally constrained radial basis function for registration and warping of images,” *Pattern Recognition Letters*, 30, 377–390, 2009.

[10] Grant, R., Schmid, M., Chiu, W., Deatherage, J., Hosoda, J., “Alignment and merging of EM images of frozen hydrated crystals,” *Biophys. J.*, 49, 251–258, 1986.

[11] J.L. Redondo, P.M. Ortigosa, I. Garcia, and J.J. Fernandez, “Image Registration in Electron Microscopy: A Stochastic Optimization Approach,” *ICIAR 2004, LNCS 3212*, pp. 141–149, 2004.

[12] M Rogers, J Graham, and R P Tonge, “2-d electrophoresis gel registration using feature matching,” In *Proceedings of the IEEE International Symposium on Biomedical Imaging*, pages 1436–1439, Arlington, USA, April 2004.

[13] K. Kaczmarek, B. Walczak, S. de Jong, and B. G. M. Vandeginste, “Matching 2D Gel Electrophoresis Images,” *J. Chem. Inf. Comput. Sci.*, *43*, 978-986, 2003.

[14] Carlos Ó. S. Sorzano, Philippe Thévenaz, and Michael Unser, “Elastic Registration of Biological Images Using Vector-Spline Regularization,” *IEEE Transactions on Biomedical Engineering*, VOL. 52, NO. 4, APRIL 2005.

[15] Buhmann, Martin D., “Radial Basis Functions: Theory and Implementations,” *Cambridge University Press*, 2003.

[16] Jasmin Blanchette, Mark Summerfield, “C++ GUI Programming with Qt4 Second Edition,” *Prentice Hall*, 2008.